Journal of Thermal Analysis and Calorimetry, Vol. 90 (2007) 1, 39–47

ROLE OF STRUCTURAL AND MACROCRYSTALLINE FACTORS IN THE DESOLVATION BEHAVIOUR OF CORTISONE ACETATE SOLVATES

S. Petit[*]*, F. Mallet, M.-N. Petit and G. Coquerel*

Unité de Croissance Cristalline et de Modélisation Moléculaire (UC^2M^2), Sciences et Méthodes Séparatives (SMS)
UPRES EA 3233, IRCOF, Université de Rouen, rue Tesnière, F-76821 Mont Saint-Aignan Cedex, France

A combined analysis of structural data and experimental results (DSC, temperature-resolved XRPD and hot stage optical microscopy) revealed that the dehydration mechanism of cortisone acetate monohydrate (CTA·H_2O) involves a collective and anisotropic departure of water molecules followed by a cooperative structural reorganization toward the anhydrous polymorph CTA (form 2). In spite of the lack of crystal structure data, it can be postulated from experimental data that thermal decomposition of the dihydrated form (CTA·$2H_2O$) and of the tetrahydrofuran solvate (CTA·THF) toward another polymorph (CTA (form 3)) also proceeds according to a cooperative mechanism, thus giving rise to probable structural filiations between these crystalline forms of CTA. The crystal structure determination of two original solvates (CTA·DMF and CTA·DMSO) indicates that these phases are isomorphous to the previously reported acetone solvate. However, their desolvation behaviour does not involve a cooperative mechanism, as could be expected from structural data only. Instead, the decomposition mechanism of CTA·DMF and CTA·DMSO starts with the formation of a solvent-proof superficial layer, followed by the partial dissolution of the enclosed inner part of crystals.

Hot stage optical microscopy observations and DSC measurements showed that dissolved materials (resulting from a peritectic decomposition) is suddenly evacuated through macroscopic cracks about 30°C above the ebullition point of each solvent. From this unusual behaviour, the necessity to investigate rigorously the various aspects (thermodynamics, kinetics, crystal structures and physical factors) of solvate decompositions is highlighted, including factors related to the particular preparation route of each sample.

Keywords: *crystal structure, desolvation mechanism, solid–solid transformation, solvates*

Introduction

Solid-solid transformations have constituted a highly active research field all along the 20th Century, involving a wide range of physical phenomena such as solid state decompositions (including dehydrations and desolvations), polymorphic transitions [1, 2], mechanical activation [3, 4], amorphization and vitrification [5], etc. Among these domains, dehydration studies of crystal hydrates often consisting of inorganic salts (e.g $CuSO_4·5H_2O$, $NiSO_4·7H_2O$, aluns, oxalates) led to develop theoretical approaches mainly derived from kinetic investigations. Although diffusion-controlled reactions and 'soft' decompositions were envisaged [6–8], the most developed concept used to describe dehydration mechanisms was nucleation and growth [9, 10]. The relationships between this model, the factors governing the kinetics of dehydration, and the associated mechanisms were for instance discussed by Lyakhov and Boldyrev [11]. In the 90's, Galwey *et al.* have also used kinetic data to describe dehydration processes of inorganic crystal hydrates, leading in particular to develop more accurately the concept of progression of a reaction interface [12–14], first described in 1916 by Langmuir [15].

In the 80's and 90's, the interest of scientists moved toward solid state organic chemistry, including the understanding of crystallization, stability, physical characterization, mechanical activation and decomposition of organic and molecular crystals [16–20]. This evolution was facilitated by technological and computational progresses, allowing much easier crystal structure determinations of molecular compounds and of organic solvates [21, 22]. Based on a combination of structural and thermomicroscopic data, Byrn proposed in 1982 one of the first rational approach of dehydration of pharmaceutical compounds [23]. Structural classifications of hydrates/solvates, together with the analysis of thermal and physical behaviours [24, 25], were shown to provide useful tools for the understanding of desolvation processes of stoichiometric or non-stoichiometric organic solvates [26, 27], and dehydration/desolvation studies of molecular compounds constitute nowadays an active research area [28, 29].

* Author for correspondence: samuel.petit@univ-rouen.fr

1388–6150/$20.00

Akadémiai Kiadó, Budapest, Hungary
Springer, Dordrecht, The Netherlands

In 1996, an extended analysis of an experimental study of solid–solid transformations based on a combination of structural data, molecular modelling, thermal analysis, electron microscopy and physical characterization, allowed some of us to propose a global model of dehydration mechanisms of molecular compounds [30]. It was assumed in this model that 'cooperative-type' or 'nucleation and growth-type' processes could probably be determined by a set of criteria related to crystal lattice features of the initial phase (hydrate) and to the evolution of the physical state of the sample in terms of size and long range order in particles resulting from the departure of water molecules. Our dual approach led to propose the concept of structural filiation, or transmission of structural information, as a key issue of dehydration mechanisms. Further studies carried out in the frame of this assumption revealed that both the research of new polymorphic forms [31] and the achievement of solvent exchanges [32, 33] could be envisaged from the understanding of desolvation mechanisms at a molecular scale.

However, our investigations also highlighted some intrinsic limitations of a model mainly derived from structural data, leading to the necessity to perform further experimental studies in order to get a wider knowledge about desolvation behaviours. The present paper belongs to this evolution and illustrates the extension of our previous ideas. It is devoted to cortisone acetate (CTA hereafter, Fig. 1), a synthetic glucocorticoid known since the 50's [34] and used as a pharmaceutical ingredient for its anti-inflammatory or immunosuppressant properties. Several crystalline phases, including three polymorphic forms, a monohydrate, a dihydrate as well as methanol, ethanol, propanol, isopropanol, acetone, methylethylketone, dioxane, tetrahydrofuran and diethylether solvates of CTA were identified and characterized by X-ray powder diffraction (XRPD), differential scanning calorimetry (DSC), infrared spectroscopy (IR) or thermomicroscopy [35–39]. Crystal structures of two polymorphs (forms 1 and 2, both orthorhombic $P2_12_12_1$), of the monohydrate (orthorhombic $P2_12_12_1$, isomorphous to the methanol solvate) and of the acetone solvate (monoclinic $P2_1$, isomorphous to the ethanol solvate) were published [40–43]. In 1972, it was assumed that the kinetics of thermal dehydration of the so-called 'unstable monohydrate' involved a succession of two polymorphic transformations after the departure of water molecules [44], whereas the desolvation mechanism of light alcohol solvates was described as a 2-dimensional growth of nuclei, according to a more recent kinetic study using the Avrami–Erofeev equation [39]. Surprisingly, these authors also showed that powders recovered by desolvation exhibited large specific surface areas and pore volumes, which could be an indicator of a cooperative and non fully destructive mechanism, rather than of a nucleation and growth process.

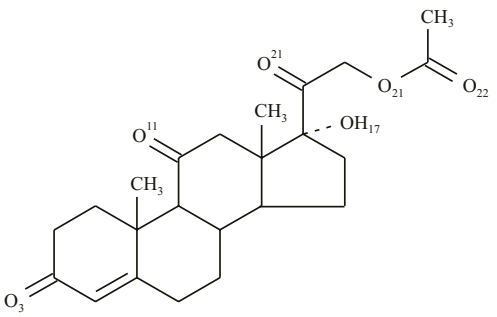

Fig. 1 Developed formula of cortisone acetate and atom numbering of oxygen atoms

In this context, and owing to the propensity of CTA to form solvates and polymorphs, our aim was to investigate the desolvation behaviour of CTA solvates by means of a combination of relevant techniques in order to propose a satisfactory interpretation of experimental observations, and to correlate this knowledge, when possible, with structural data. Due to the large number of identified CTA solvates, only pertinent or representative cases are reported here.

Experimental

Materials

Cortisone acetate (CTA) was kindly supplied in its monohydrated form by Sanofi-Aventis. Single crystals of this hydrate ($CTA{\cdot}H_2O$) were obtained by slow evaporation at room temperature of a saturated solution in a methanol/water mixture (70:30 *v*/*v*), and no mixed solvate ($CTA{\cdot}MeOH_x{\cdot}H_2O_{1-x}$) was obtained in these conditions. The dihydrated form ($CTA{\cdot}2H_2O$) was produced by precipitation resulting from the rapid addition of water to a methanolic solution of CTA under stirring (final ratio $MeOH/H_2O$ 1:4), but could also be obtained by grinding in an aqueous suspension. The tetrahydrofuran solvate (CTA·THF) resulted from THF evaporation of a saturated solution. Crystals of dimethylformamide and dimethylsulfoxide solvates (CTA·DMF and CTA·DMSO, respectively) were obtained by cooling to room temperature saturated solutions prepared with the corresponding solvents.

Characterization techniques

Crystalline phases were identified by means of X-ray powder diffraction (XRPD), with a Siemens D5005 diffractometer equipped with a copper source. All XRPD measurements were carried out in ambient at-

mosphere. For temperature-resolved XRPD, the heating rate was 2 K min^{-1}, and the recording time was about 40 min in isothermal conditions.

DSC experiments were performed using a Setaram DSC 141 apparatus. Smoothly ground samples (from 15 to 20 mg) were introduced in non covered aluminium crucibles and heated in ambient atmosphere at a 2 K min^{-1} heating rate. Samples were weighed after each DSC analysis.

Thermally-induced physical transformations of single crystals were also investigated in ambient atmosphere by using a hot stage optical microscope equipped with a digital camera, in a magnification range varying from 20 to 100, at a 2 K min^{-1} heating rate.

The CTA/solvent stoichiometries of solid samples were determined from ^{1}H-NMR analyses performed in DMSO-d6 with a Bruker Avance 300 (300 MHz) spectrometer.

Structural investigations

Crystal structures of CTA·DMF and CTA·DMSO were determined at 293 K by X-ray diffraction measurements using a Smart Apex system (Bruker) equipped with a CCD detector and a MoK_α source (λ=0.71073 Å). A structure solution was obtained with direct methods and atomic coordinates were refined with the SHELX-5.10 program [45].

Results and discussion

Dehydration behaviour of cortisone acetate monohydrate

Characterization and dehydration of CTA monohydrate

The DSC analysis of CTA·H_2O shown in Fig. 2 indicates that dehydration starts at ca. 60°C and is completed at 90°C. It can be deduced from this rather low dehydration temperature that water molecules are probably not strongly involved in the crystal cohesion, nor encaged in cavities of the crystal lattice. The shoulder observed between 60 and 70°C could be due to the sample preparation inducing a heterogeneous

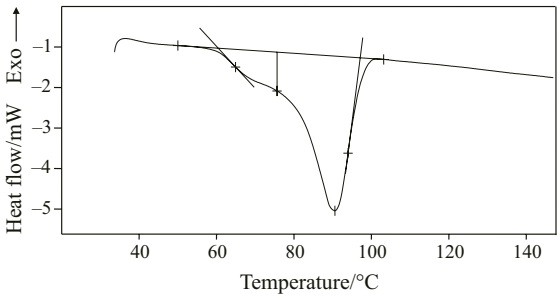

Fig. 2 DSC curve of CTA·H_2O (heating rate 2 K min^{-1})

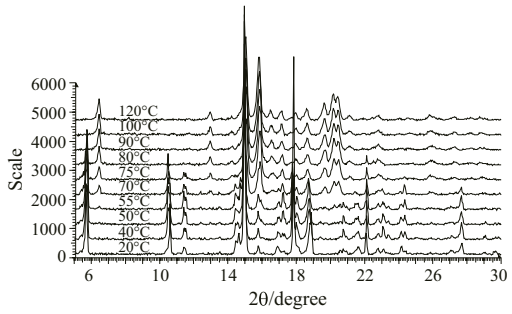

Fig. 3 Temperature-resolved XRPD analysis of CTA·H_2O between 20 and 120°C showing the progressive transformation into CTA (form 2)

crystal size distribution and crystallinity, or to an intermediate phase produced by the dehydration process. However, a temperature-resolved XRPD analysis performed between 30 and 120°C (Fig. 3) did not allow to identify any intermediate crystalline compounds, since the only new phase detected from 55°C upwards is the anhydrous CTA (form 2). The temperature gap (ca. 5–10°C) between DSC and XRPD analyses results from the supplementary isothermal step (about 40 min) required for pattern recording during temperature-resolved XRPD experiments. The simultaneous existence of CTA·H_2O and CTA (form 2) between 55 and 80°C reveals that dehydration proceeds probably by means of a progressive and smooth mechanism, without disruption of the initial crystal lattice. This statement was reinforced by hot stage microscopy (HSM) observations (Fig. 4) showing that the crystal shape and integrity is preserved along the thermal treatment. The only detectable effect of dehydration is the appearance and the development of dark zones often located on macroscopic defects of the initial particles, and inducing, after complete dehydration, a significant loss of transparency.

Structural approach and mechanism of CTA·H_2O dehydration

From the above results, it can be stated that thermally-induced dehydration of CTA·H_2O occurs at moderate temperature, without entire disruption of

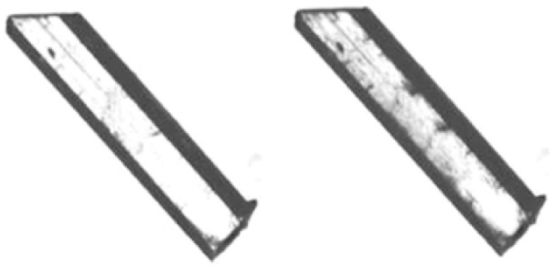

Fig. 4 Hot stage optical microscopy photographs showing the evolution of a single crystal during the dehydration of CTA·H_2O, left: 20°C; right: 70°C

the crystal lattice or existence of a long lasting intermediate amorphous state, and proceeds rather homogeneously in the sample, probably starting in the vicinity of defects since macroscopic consequences of dehydration were observed by the appearance of defective zones in single crystals. These data suggest a non destructive, cooperative dehydration mechanism, probably involving, after the departure of water molecules, a structural reorganization through cooperative molecular movements of limited magnitude.

This hypothetical mechanism is confirmed by the comparison of structural features in the crystal packings of CTA·H_2O [43] and CTA (form 2) [40]. Despite slightly different molecular orientations, the similarity between the two packings consisting of high density (002) slices appears in Fig. 5, as well as the different packing existing in CTA (form 1) [41]. It can also be seen from this figure that the reorganization step should involve a glide of (002) slices along the *b* direction, with a magnitude close to *b*/2, probably concomitant with molecular rotations of about 15° (Fig. 6).

This preliminary global comparison of structural features provides a starting point from which a more detailed structural analysis of the dehydration mechanism of CTA·H_2O can be envisaged, dealing in particular with hydrogen bonding patterns and with the description of the easiest (and therefore most probable) pathway for the release of water molecules. In the structure of CTA·H_2O, water molecules are located between (002) slices, and, owing to the size of structural channels along the *a* and *b* crystallographic axes, are more likely to be progressively evacuated along the *a* direction. This statement was readily deduced from a comparison of space-filling representations performed with the Cerius[2] molecular modelling software (data not shown). Concerning H-bonding patterns, each water molecule in the hydrated packing participates to three hydrogen bonds with three different CTA molecules located in neighbouring (002) slices, a strong H-bond involving the OH(17) group ($d(O_{17}–O_{H_2O})$=2.74Å) and two weaker H-bonds in which the water molecule acts as a donor group: $d(O_3–O_{H_2O})$=2.87Å and $d(O_{20}–O_{H_2O})$=2.96Å (Fig. 6, left) [43]. The departure of water molecules obviously implies the disruption of these H-bonds, and the OH(17) group remains as the only H-bond donor. In the crystal structure of CTA (form 2), the intermolecular H-bond involves the O(17) and O(22) oxygen atoms, corresponding to [010] molecular ribbons (Fig. 6, right) [40], and it is of interest to notice that, in 'dehydrated CTA·H_2O' (i.e. just after the departure of water molecules), the distance between these atoms corresponds to the shortest distance between the donor group OH(17) and an oxygen atom (Fig. 6, middle). It can be deduced from these structural data that the reorganization step, after the evacuation of water from the crystal lattice, involves a stabilization of the resulting packing through cooperative movements allowing the formation of a new intermolecular H-bond along [010]. Together with the above mentioned results, this analysis (performed on 'ideal' crystals deprived of any defect) provides a supplementary argument in favour of a cooperative dehydration mechanism of CTA·H_2O, inducing the probable existence of a structural filiation between CTA·H_2O and CTA (form 2). Although the reversibility of this dehydration was not investigated experimentally, the above statements suggest that rehydration should also occur in a cooperative way.

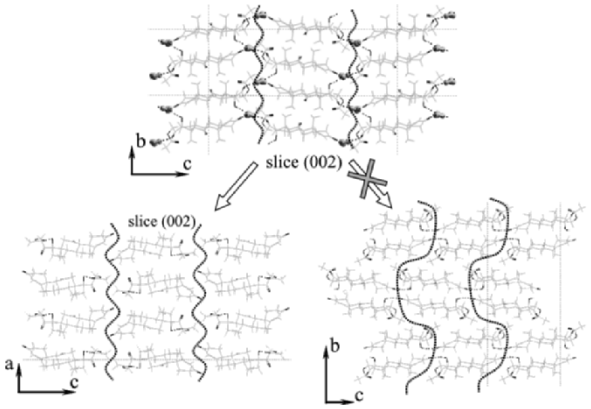

Fig. 5 Projections along the shortest axes for CTA·H_2O (upper), CTA (form 2) (lower-left) and CTA (form 1) (lower-right) crystal structures

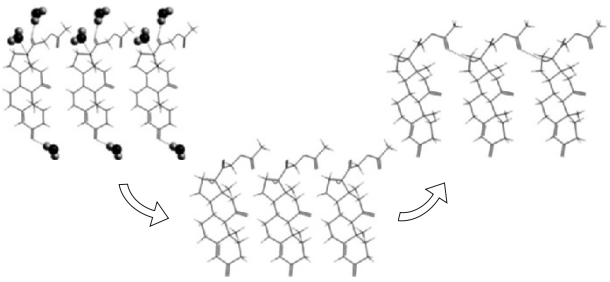

Fig. 6. Representation of hydrogen bonds in the structures of CTA·H_2O (left) and CTA (form 2) (right). A hypothetical intermediate situation (dehydrated CTA·H_2O) is also represented (middle)

Behaviour of cortisone acetate dihydrate and of the THF solvate

Distinct hydrated phases of CTA, presenting specific IR spectra and DSC curves, were previously mentioned in the literature [36]. The importance of solvent composition, especially its water content, was emphasized for the preparation of different solvated or hydrated phases, but their stoichiometries were not always clearly established.

The crystalline form produced by precipitation in a methanol/water mixture was shown to present an original XRPD pattern, compared to that of CTA·H_2O (Fig. 7), and its dehydration, characterized by DSC, was shown to occur in the temperature range 35–40°C (Fig. 8), i.e. at a much lower temperature than for the monohydrate. Furthermore, the mass loss associated to dehydration was about 8.3%, establishing that this form is a dihydrate (calc. 8.21%).

Attempts to prepare single crystals of CTA·$2H_2O$ were unsuccessful, so the study of its dehydration behaviour could only be performed by temperature-resolved XRPD. These data, shown in Fig. 9, revealed that, interestingly, dehydration results in the formation of CTA (form 3), and this anhydrous polymorph is the only detected phase between 35 and 80°C.

A similar behaviour was observed for the tetrahydrofuran solvate of CTA (CTA·THF, see XRPD pattern in Fig. 7), but its thermal desolvation proceeds in a much widespread temperature range, since the first diffraction peaks of CTA (form 3) appear at about 40°C, whereas CTA·THF is no longer detected at 80°C (data not shown). This is consistent with the DSC curve obtained with this solvate, exhibiting a widespread endothermic phenomenon between ca. 50 and 100°C, with a maximum close to 75°C (Fig. 8, middle). The (1:1) stoichiometry of this solvate was assessed by both ^{1}H-NMR spectroscopy and gravimetric measurements (exp. mass loss: ca. 15; calc. 15.2%).

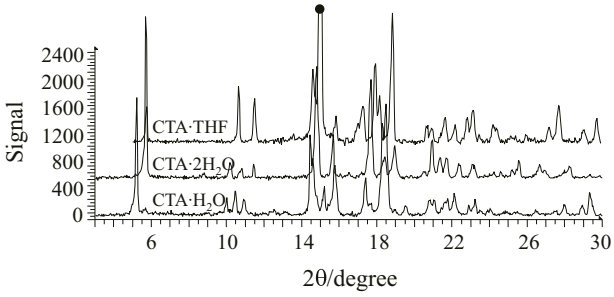

Fig. 7 XRPD patterns of CTA·H_2O (lower), CTA·$2H_2O$ (middle) and CTA·THF (upper)

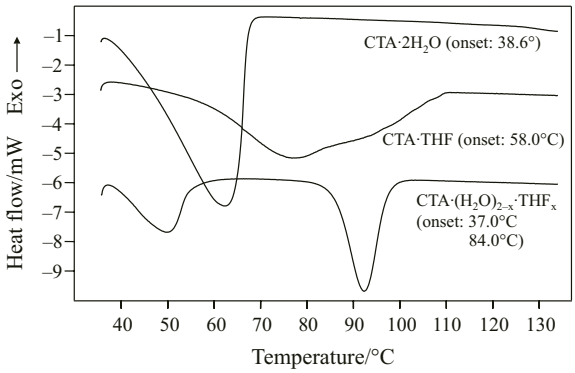

Fig. 8 DSC curve of CTA·$2H_2O$ (upper), CTA·THF (middle) and of partially hydrated CTA·THF under ambient RH (lower)

The similarity between the desolvation behaviours of CTA·$2H_2O$ and CTA·THF suggests that structural resemblances might exist between these two solvates, and also probably with CTA (form 3).

Although it cannot be stated from XRPD patterns that these forms are isomorphous, the hypothesis of structural similarities was reinforced by equilibration studies under various residual humidities (RH) at room temperature. It was observed that CTA (form 3) produced either by dehydration of CTA·$2H_2O$ or desolvation of CTA·THF is fully rehydrated into CTA·$2H_2O$ after seven days under 100% RH at room temperature. It also appeared that crystals of CTA·THF maintained for several days under atmospheric humidity at 20°C undergo a spontaneous transformation toward CTA·$2H_2O$, as confirmed by XRPD and gravimetric analysis (mass loss: 13.4% after two days). The assumed stoichiometry for this mixed solvate is therefore CTA·$(H_2O)_{2-2x}$·$(THF)_x$ ($0 \le x \le 1$), but it cannot be established, owing to its DSC behaviour (Fig. 8, lower), that this phase constitutes a homogeneous solid solution since two distinct thermal events can be contemplated, namely a dehydration at ca. 37°C and a desolvation starting at about 80°C. Compared to the 'pure' THF solvate (Fig. 8, middle), the reason for the well-defined shape of the desolvation phenomenon of CTA·THF after equilibration is likely to be due to the different vapour pressures of the two solvents in this temperature range.

Despite the absence of structural data, the reversibility of CTA·$2H_2O$ dehydration and CTA·THF desolvation is a strong indicator that structural filiations may exist between these solvates and CTA (form 3), and suggests, despite significant differences in their XRPD patterns, that this non solvated form could be close to an isomorphic desolvate [27]. Indeed, dehydration or desolvation toward the higher melting point CTA (form 1) [35] was never observed, and rehydration under ambient or 100% RH did not induce the formation of the 'more stable' monohydrated form of CTA.

Hence, this study illustrates that, despite the absence of structural data, some assumptions about the desolvation mechanism of molecular compounds can be deduced from a careful experimental investigation of solid–solid transformations between well-identified forms. Such analysis must take into account the reversibility of transformations and the spontaneous evolution of crystalline phases under controlled atmosphere, possibly leading to mixed or non stoichiometric solvates [46].

Desolvation behaviour of DMF and DMSO solvates of cortisone acetate

Structural features of CTA·DMF and CTA·DMSO

Despite a similar skeleton, steroids can present very different solubility values in non volatile solvents such as dimethylformamide (DMF) and dimethylsulfoxide (DMSO). For instance, the solubility of dexamethasone acetate at room temperature in these solvents ranges from 30 to 35% mass/mass% [33], whereas CTA presents very low solubilities at 20°C, 0.60 and 0.21% mass/mass% in DMF and DMSO, respectively.

In order to determine crystal structures, single crystals obtained by cooling hot saturated solutions were analysed by X-ray diffraction, from which the (1:1) stoichiometry of the two solvates could be determined. The crystallographic parameters and the main parameters of structural determinations performed at room temperature are presented in Table 1. Complete structural data were deposited at the Cambridge Crystallographic Data Center and registered under deposition numbers CCDC-623916 (CTA·DMF) and CCDC-623917 (CTA·DMSO). The relatively high R value obtained for CTA·DMSO is due to a partial disorder of solvent molecules in the crystal lattice, and idealized mean atomic coordinates have been retained for projection purposes.

The comparison of unit cell dimensions from Table 1 suggests that the two structures are isomorphous with the CTA·Acetone solvate. It can be seen from Fig. 10 that molecular conformations are almost identical, and that crystal packings are composed of high-density (001) molecular slices. Molecules are related to each other by means of a helicoidal arrangement, but do not form direct inter-

Table 1. Measurement conditions, refinement factors and crystallographic parameters for crystal structure determinations of CTA·DMF and CTA·DMSO. Crystallographic parameters of the acetone solvate of CTA are given for comparative purpose

	CTA·DMF	CTA·DMSO	CTA·acetone [42]
Formula	$C_{23}H_{30}O_6 \cdot C_3H_7ON$	$C_{23}H_{30}O_6 \cdot C_2H_6OS$	$C_{23}H_{30}O_6 \cdot C_3H_6O$
Molecular mass/g mol^{-1}	475.57	480.60	460.57
Space group	$P2_1$	$P2_1$	$P2_1$
Z	2	2	2
a/Å	9.7935(6)	9.7416(8)	9.820(2)
b/Å	7.5127(4)	7.6975(6)	7.661(5)
c/Å	16.595(1)	16.533(1)	16.648(1)
β/°	97.83(1)	94.75(1)	94.65(1)
V/Å^3	1209.6(1)	1235.4(2)	1248.3(9)
μ/mm^{-1}	0.094	0.173	0.08
Scan type	2θ	2θ	ω/2θ
Dx/g cm^{-3}	1.306	1.292	1.225
Wavelength/Å	0.71073	0.71073	0.71069
F(000)	512	516	496
θ limits/°	1.24–28.30	1.24–26.40	0–27
h, *k*, *l* range	–13/12 ; –9/9 ; 0/22	–12/12 ; –9/9 ; –20/20	–12/12 ; –9/9 ; –21/21
Nb of independent reflexions	5572	5028	2918
Nb of observed reflexions	5200 ($F_0^2>2\sigma(F_0^2)$)	2821 ($F_0^2>2\sigma(F_0^2)$)	1587 ($F_0^2>2\sigma(F_0^2)$)
Goodness of fit	1.039	0.881	–
R/*wR*$_2$/%	5.50/13.98	7.22/20.31	6.3/5.7
$\Delta\rho_{min}$, $\Delta\rho_{max}$/e Å^{-3}	–0.32, 0.38	–0.32, 0.67	–0.2, 0.2

Table 2 Geometric characteristics of CTA-solvent hydrogen bonds in the isomorphous structures of DMF, DMSO and acetone solvates

	CTA·DMF	CTA·DMSO	CTA·acetone [42]
$d(O_{17}\cdots O)$/Å	2.72	2.63	2.80
$d(OH_{17}\cdots O)$/Å	1.86	1.67	1.85
$(O_{17}–H_{17}\cdots O)$/°	179.3	179.0	179.4

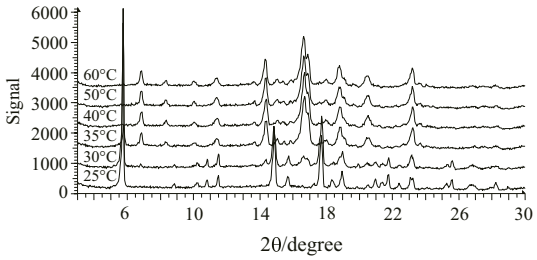

Fig. 9 Temperature resolved XRPD analysis of CTA·2H_2O between 25 and 60°C showing the transformation toward CTA (form 3)

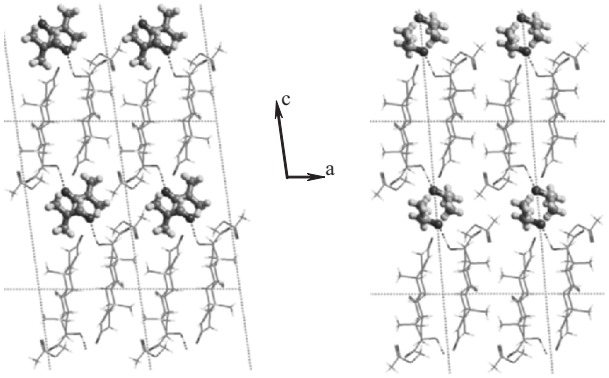

Fig. 10 Projections along the *b* axis of CTA·DMF (left) and CTA·DMSO (right) crystal structures

molecular H-bonds. The only donor group OH(17) of the CTA molecule is involved in a H-bond with solvent molecules whose geometric parameters are given in Table 2. Further details about conformational and packing features have been depicted by van Geerestein and Kanters [42].

Thermal behaviour of CTA·DMF and CTA·DMSO

Owing to the existence of large structural channels running along the *b* axis in which solvent molecules are inserted, it could be postulated from crystal structure data only that desolvation should easily proceed according to a cooperative mechanism. In the case of the acetone solvate, this hypothesis could account for the poor stability of single crystals, inducing a significant decrease of diffracted intensities under exposure to X-rays [42]. For DMF and DMSO solvates, such decreases were not observed, probably because of the poor volatility of these solvents at room temperature.

Large and well-defined single crystals of CTA·DMF and CTA·DMSO were selected in order to investigate the thermal and desolvation behaviour of these phases by hot-stage optical microscopy. In contradiction with the assumed cooperative mechanism, it was observed upon heating to ca. 140°C that the progressive loss of crystal transparency (Fig. 11) was not due to desolvation but rather to a partial transformation of the material occurring only at the surface of

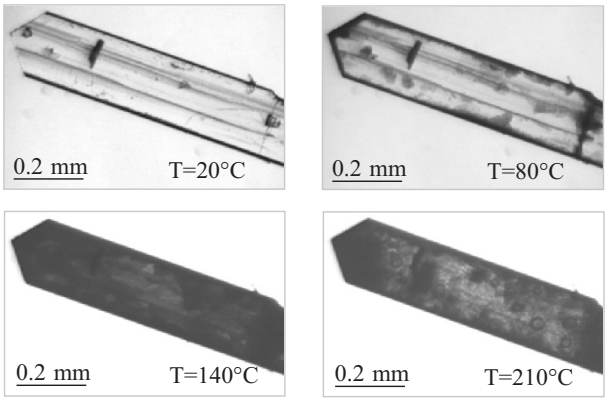

Fig. 11 Optical microscopy photographs showing the evolution of a CTA·DMSO crystal upon heating

the initial particle, and leading to the formation of a solvent-proof layer without destruction or detectable change of the crystal shape.

Between 140 and 210°C, the particle slowly recovered a partial transparency, allowing to visualize the existence of droplets probably made of saturated solution (Fig. 11, lower-right). At temperatures about 30°C above the ebullition point of the solvents (180°C for CTA·DMF and 225°C for CTA·DMSO), the amount of dissolved material and the associated increase of internal pressure in the particle led to observe the sudden evacuation of the solution through macroscopic cracks, colloquially labelled 'pop corn effect' in our laboratory (data not shown).

In order to get further information about the thermal behaviour of CTA·DMF and CTA·DMSO solvates, DSC analyses were performed in the same temperature range, leading to hardly interpretable curves such as that shown in Fig. 12. The succession of thermal events may be a combined consequence of a heterogeneity of crystal size distribution and of the above mentioned phenomena. The only unambiguous part of the DSC curve is the sudden and sharp peak observed at the end of the process (228°C for CTA·DMSO), most likely caused by the 'pop corn' effect corresponding to the escape of a saturated solution through cracks appearing at the surface of particles. As a putative interpretation of this curve, and in relation with optical microscopy data, one may assume that thermal events between ca. 30 and 115°C could correspond to the formation of the solvent-proof layer, whereas the large phenomenon detected from 125 to 200°C could be due to the progressive dissolution of the inner part of the particle.

Hence, it can be deduced from these observations that, by contrast with the spontaneous desolvation reported for the isomorphous CTA·acetone solvate [42], desolvation of CTA·DMF and CTA·DMSO involve successive physical phenomena that cannot be accounted from structural data only. In particular, the

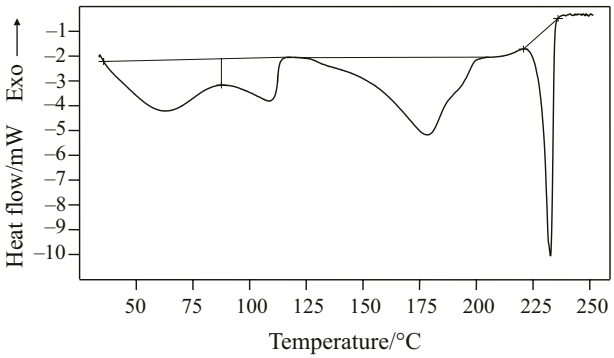

Fig. 12 DSC curve of CTA·DMSO crystals. The heating rate is 2 K min^{-1}

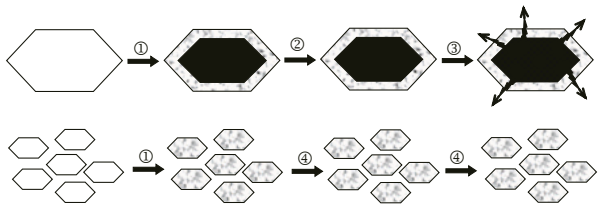

Fig. 13 Schematic representation of the assumed thermal behaviour of CTA·DMF and CTA·DMSO, and influence of particle size (① – formation of a solvent-proof layer; ② – partial dissolution of the unreacted inner part; ③ – evacuation of the saturated solution through cracks, and possible recrystallization; ④ – no evolution)

formation of a solvent-proof layer at the surface of the particles may be mainly a consequence of the low volatility of the solvents, although such phenomenon was envisaged by Galwey in the case of inorganic hydrates [14]. Regarding the partial dissolution of materials enclosed inside the particles, it can be assumed that it is made possible by the diffusion of solvent molecules encaged in the sample, caused by the increase of thermal motions upon heating. This hypothesis is reinforced, on the one hand, by the low solubility of CTA in these solvents at room temperature (although solubilities at higher temperatures have not been determined), and on the other hand, by the relatively large anisotropic displacement parameters for solvent molecules (in particular for DMSO) in the crystal structures determined at 20°C. It should also be mentioned that a related behaviour during thermal desolvation has been reported by Petropavlov for the DMSO solvate of another steroid, cortexolone [47]. In this case, however, polarization microscopy observations revealed the formation of DMSO drops at the surface of the initial particle, from which a non solvated crystalline form of cortexolone could nucleate and grow, depending on kinetic conditions.

More generally, this type of phenomena relies to the incongruent melting of solvates [48], obviously more often encountered in the case of poorly volatile solvents such as DMF or DMSO, but also NMP (*N*-methylpyrrolidinone) [31]. In the case of the CTA solvates studied here, another major parameter is the size of the analysed crystals, since partial dissolution of enclosed material can only be observed if particles are large enough. As illustrated in Fig. 13, the evolution of samples composed of too small particles may be limited to a solid–solid transformation (direct desolvation, possibly by a nucleation and growth mechanism), which may give rise to difficulties in attempts to propose a consistent interpretation of data collected by means of different techniques. In consistency with results presented here, the influence of particle size on solid-solid reactions of inorganic compounds and their kinetics has been illustrated and analysed by Feitknecht [49], showing that the magnitude of this effect is also determined by desolvation or decomposition mechanisms [50].

Conclusions

In combination with thermal analysis, optical microscopy and complementary characterization techniques, structural data are powerful tools for the elucidation of dehydration or desolvation mechanisms of molecular crystals. However, the results presented here show that predictions based on crystal structures only are clearly insufficient since many physical parameters can modify or at least significantly alter the decomposition mechanism of solvates as well as their kinetics. In the case of cortisone acetate, it appeared that factors such as the nature of the solvent and its volatility, the relative stability of the solvate *vs*. residual humidity, the crystal size distribution and the physical heterogeneity of the sample, including crystal defects, could have major consequences on the thermal behaviour of various solvates.

As a consequence, it can be suggested that three distinct groups of factors should be considered for a satisfactory approach of desolvation phenomena. The first one involves thermodynamic aspects, and is correlated, in particular, to the relative stability of solid phases as a function of temperature, relative humidity and composition of the system. The second group includes structural aspects and crystal lattice features, whereas the third one (last but not least) deals with numerous physical factors often determined by the preparation route of each sample (size, shape, defects, etc.) that can affect the desolvation behaviour. Since parameters of this third group were often ignored in previous investigations, further studies aiming at analysing the specific consequences of physical factors on the desolvation of molecular crystals should be performed and incorporated in interpretation efforts.

Acknowledgements

This work was made possible thanks to CRIHAN (Centre de Ressources Informatiques de Haute-Normandie) which provided access to molecular modelling tools allowing the analysis of crystal structures. Sanofi-Aventis is acknowledged for providing a financial support to F. Mallet. Thanks are also due to Dr. Fabrice Dufour for his contribution to crystal structure determinations.

References

1 Yu. V. Mnyukh, Mol. Cryst. Liq. Cryst., 52 (1979) 163.
2 T. L. Threlfall, Analyst, 120 (1995) 2435.
3 R. Hüttenrauch, S. Fricke and P. Zielke, Pharm. Res., (1985) 302.
4 V. V. Boldyrev, J. Mater. Sci., 39 (2004) 5117.
5 S. Petit and G. Coquerel, Polymorphism in the Pharmaceutical Industry, R. Hilfiker, Ed., Wiley-VCH, Weinheim, Germany 2006, p. 259.
6 R. W. Munn, Chem. Brit., 14 (1978) 231.
7 N. Boudjada, J. Rodriguez-Carvajal, M. Anne and M. Figlarz, J. Solid State Chem., 105 (1993) 211.
8 L. Stoch, J. Thermal Anal., 38 (1992) 131.
9 J.-C. Niepce and G. Watelle-Marion, C. R. Acad. Sci., 276 (1973) 627.
10 A. K. Galwey and G. M. Laverty, J. Chim. Phys., 87 (1990) 1207 and references therein.
11 N. Z. Lyakhov and V. V. Boldyrev, Russ. Chem. Rev., 41 (1972) 919.
12 A. K. Galwey, J. Thermal Anal., 38 (1992) 99.
13 A. K. Galwey, Proc. R. Soc. London A, 441 (1993) 313.
14 A. K. Galwey, Thermochim. Acta, 355 (2000) 181.
15 I. Langmuir, J. Am. Chem. Soc., 38 (1916) 2221.
16 S. R. Byrn, R. R. Pfeiffer, M. Ganey, C. Hoiberg and G. Poochikian, Chem. Mater., 6 (1994) 1148.
17 D. Giron, Thermochim. Acta, 248 (1995) 1.
18 N. Rodriguez-Hornedo and D. Murphy, J. Pharm. Sci., 88 (1999) 651.
19 A. K. Galwey, J. Pharm. Pharmacol., 51 (1999) 879.
20 T. P. Shakhtshneider and V. V. Boldyrev, Reactivity of Molecular Solids, E. Boldyreva, V. V. Boldyrev, Eds, Wiley & Sons, New York 1999, p. 271.
21 P. Van der Sluis and J. Kroon, J. Cryst. Growth, 97 (1989) 645.
22 C. H. Görbitz and H. P. Hersleth, Acta Cryst., B56 (2000) 526.
23 S. R. Byrn, Solid-State Chemistry of Drugs, Academic Press, New York 1982, p. 149.
24 R. K. Khankari and D. J. W. Grant, Thermochim. Acta, 248 (1995) 61.
25 D. Giron, C. Goldbronn, M. Mutz, S. Pfeffer, P. Piechon and P. Schwab, J. Therm. Anal. Cal., 68 (2002) 453.
26 K. R. Morris, Polymorphism in Pharmaceutical Solids, H. G. Brittain, Ed., Marcel Dekker Inc., New York 1999, p. 125.
27 G. A. Stephenson, E. G. Groleau, R. L. Kleemann, W. Xu and D. R. Rigsbee, J. Pharm. Sci., 87 (1998) 536.
28 M. D. Jones, J. C. Hooton, M. L. Dawson, A. R. Ferrie and R. Price, Int. J. Pharm., 313 (2006) 87.
29 H. J. Zhu, Int. J. Pharm., 315 (2006) 18.
30 S. Petit and G. Coquerel, Chem. Mater., 8 (1996) 2247.
31 S. Garnier, S. Petit and G. Coquerel, J. Therm. Anal. Cal., 68 (2002) 489.
32 F. Mallet, S. Petit, S. Lafont, P. Billot, D. Lemarchand and G. Coquerel, J. Therm. Anal. Cal., 73 (2002) 459.
33 F. Mallet, S. Petit, S. Lafont, P. Billot, D. Lemarchand and G. Coquerel, Cryst. Growth Des., 4 (2004) 965.
34 E. S. Rothman and M. E. Wall, J. Am. Chem. Soc., 81 (1959) 411.
35 R. K. Callow and O. Kennard, J. Pharm. Pharmacol., 13 (1961) 723.
36 J. E. Carless, M. A. Moustafa and H. D. C. Rapson, J. Pharm. Pharmacol., 18 (1966) 190.
37 M. Kuhnert-Brandstätter and H. Grimm, Mikrochim. Acta, (1968) 115.
38 R. J. Mesley, J. Pharm. Pharmacol., 20 (1968) 877.
39 K. Shirotani and K. Sekiguchi, Chem. Pharm. Bull., 29 (1981) 2983.
40 J. P. Declercq, G. Germain and M. Van Meerssche, Cryst. Struct. Commun., 1 (1972) 59.
41 J. A. Kanters, A. de Koster, V. J. van Geerestein and L. A. van Dijck, Acta Cryst. C., 41 (1985) 760.
42 V. J. van Geerestein and J. A. Kanters, Acta Cryst. C., 43 (1987) 136.
43 V. J. van Geerestein and J. A. Kanters, Acta Cryst. C., 43 (1987) 936.
44 J. E. Carless, M. A. Moustafa and H. D. C. Rapson, J. Pharm. Pharmacol., 24 (1972) 130P.
45 G. M. Sheldrick, SHELXTL, Release 5.10, (Program for the determination and the refinement of crystal structures), Bruker Analytical X-ray Instruments Inc., Madison, Wisconsin, USA.
46 U. J. Griesser, Polymorphism in the Pharmaceutical Industry (ed. R. Hilfiker), Wiley-VCH, Weinheim, Germany 2006, p. 211.
47 N. N. Petropavlov, J. Cryst. Growth, 52 (1981) 889.
48 J. E. Ricci, The Phase Rule and Heterogeneous Equilibrium, Dover Publications, New York 1966, p. 278.
49 W. Feitknecht, Pure Appl. Chem., 9 (1964) 423.
50 R. Giovanoli, H. R. Oswald and W. Feitknecht, Helv. Chim. Acta, 49 (1966) 1971.

DOI: 10.1007/s10973-007-8475-z